Comparative Molecular Field Analysis (CoMFA) of Anionic Azo Dye-Fiber Affinities I: Gas-Phase Molecular Orbital Descriptors

Simona Funar-Timofei*

Institute of Chemistry, Romanian Academy, Bul. Mihai Viteazul 24, 1900 Timisoara, Romania

Gerrit Schüürmann

Department of Chemical Ecotoxicology, UFZ Centre for Environmental Research, Permoserstr. 15, D-04318 Leipzig, Germany

Received August 20, 2001

This paper presents quantitative structure−activity relationship (QSAR) models for a series of 30 anionic azo dyes applied to cellulose fiber by comparative molecular field analysis. Two forms of the dye molecules (neutral and anionic) are compared. Neutral structures give better statistical results than the anionic species. The electronic and structural properties of these dyes were calculated by the semiempirical AM1 method. The results indicate the predominance of electrostatic interactions in dye-cellulose binding. The dominant contribution of the HOMO orbital molecular energy, used as descriptor, can be explained by the donor ability of the dye molecules in the dye adsorption on cellulose.

INTRODUCTION

QSAR-type studies for dye-cellulose fiber interaction have been applied in the last years in the study of dye adsorption on cellulose fiber.[1−10] A series of anthraquinone vat dyes, mono, bisazo, and disperse dyes, were studied by several variants of classical QSAR, 3D-QSAR, and by other modern methods. They demonstrated at least an appreciable similarity of dye-fiber interactions with receptor−ligand interactions.[10]

The arguments for the application of QSAR techniques in dye adsorption on cellulose come from both the variety of data of the physical chemistry of dyeing and the complexity of the cellulose fiber structure.[10]

As an alternative to classical QSAR studies, comparative molecular field analysis (CoMFA)[11] was used to predict technical dye adsorption properties. This method was applied to a series of anthraquinone vat dyes,[7] symmetrical bisazo dyes,[8] and heterocyclic monoazo dyes.[12] Electrostatic dye-fiber interactions have been found to dominate the steric ones. The LUMO orbital molecular energy used as a descriptor[7,12] had a dominant contribution in the process of dye adsorption on fiber. Perhaps the most interesting result, as indicated mainly by CoMFA studies concerning the contribution of electrostatic fields, is that an increase of positive charges in the dye molecule favors dye adsorption on cellulose.[10]

In a previous CoMFA study applied to disperse azo dyes, the dye binding to cellulose seemed to be less specific in terms of pharmacophoric constraints.[9] Some recent results published by Woodcock point to the specific adsorption of the anionic azo dye Congo Red on the crystalline cellulose surfaces.[13] Experimental arguments are mentioned according to which dye molecules are adsorbed in monomeric form on microcrystalline cellulose into the interlinking region between elementary crystallites, penetrating into them from both ends are noticed.[14] Kai et al.[15,16] studied the effects of some direct dyes on microbial cellulose by X-ray diffraction, solid state ^{13}C NMR, and deuteration-IR determinations. They concluded that these dyes formed a product with the microbial cellulose which is a crystalline complex composed of a dye and cellulose.

The binding site for the dye molecule was considered to be situated in the crystalline region of the cellulose, in the "holes" resulted from the supramolecular structure.[17] The dimensions of these sites between the micro- and macrofibrils are of the order of a few angströms or more.[18]

Adsorption on cellulose and lipophilicity of a series of anionic azo dyes was studied by multiple linear regression, principal component regression, and minimal steric difference method.[5] It was concluded that adsorption of anionic azo dyes by cellulose depended mainly on steric and to a lesser extent on electronic interactions (expressed by hydrogen bonding ability). Hydrophobic effects were observed only in the fiber sorption of subseries of dyes having the coupling component with one and two, respectively, sulfonic acid groups.

To get new insights on the effects of the structural modifications of the same series of 30 anionic azo dyes[19] the CoMFA method was applied to study the dye ability to bind to cellulose fibers. Additional semiempirical molecular orbital (AM1) calculations have been performed to develop low-energy conformations and QSAR descriptors. Experimental dye affinities and quantum chemical descriptors are presented in Table 1.

COMPUTATIONAL DETAILS

Starting structures were generated using the SYBYL package,[20] with the TRIPOS force field,[21] and quantum-mechanics have been performed for the molecular lowest energy calculations. Molecular geometries were determined starting from crystallographic information. The −N═N−

* Corresponding author fax: +40-56-191824; e-mail: timofei@acad-tim.utt.ro.

10.1021/ci010086v CCC: $22.00
Published on Web 06/04/2002

Table 1. Experimental Dye Affinity ($-\Delta\mu^o$) and Quantum-Mechanics AM1 Results of Anionic Azo Dyes (I) Included in the CoMFA Model I (Alignment Model 3)

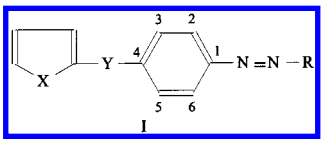

I

no.	X	Y	R[a]	$-\Delta\mu^o$ (kJ/mol)	E_{HOMO}[b] (eV)	E_{LUMO}[b] (eV)	L[b] (Å)	ClogP[b]	ΔH[b] (kJ/mol)
1	-S-	-CH = CH-	A	15.80	−8.45	−1.26	17.61	4.608	−157.6
2	-CH = CH-	-CH = CH-	A	14.25	−8.53	−1.23	17.99	4.962	−157.4
3	-S-	-CONH-	A	13.08	−8.49	−1.13	17.62	3.117	−153.5
4	-CH = CH-	-CONH-	A	12.00	−8.49	−1.13	17.91	3.379	−153.8
5	-S-	-CH = CH-	B	9.66	−8.64	−1.49	17.49	5.212	−172.7
6	-S-	-CH = CH-	C	9.45	−8.63	−1.91	19.88	2.292	−686.32
7	-CH = CH-	-CH = CH-	B	9.20	−8.75	−1.49	17.91	5.566	−210.7
8	-S-	-CONH-	C	9.03	−8.62	−1.79	19.97	0.686	−849.15
9	-S-	-CO-	A	8.78	−8.87	−1.35	15.63	3.506	−164.4
10	-CH = CH-	-CH = CH-	C	8.40	−8.64	−1.88	20.32	2.646	−698.31
11	-CH = CH-	-CONH-	C	8.28	−8.68	−1.82	20.28	0.949	−877.71
12	-S-	-CONH-	B	7.15	−8.79	−1.38	17.52	3.72	−168.90
13	-S-	-CH = CH-	D	7.06	−8.66	−2.04	19.81	2.862	−864.94
14	-CH = CH-	-CO-	A	7.02	−8.88	−1.31	15.93	3.767	−165.00
15	-CH = CH-	-CONH-	B	6.52	−8.79	−1.38	17.85	3.983	−169.10
16	-S-	-CH = CH-	E	6.27	−8.75	−1.96	18.08	3.355	−684.83
17	-S-	-CONH-	D	6.23	−8.79	−1.87	19.86	1.249	−1043.55
18	-CH = CH-	-CH = CH-	D	6.02	−8.88	−2.08	20.32	3.216	−886.31
19	-CH = CH-	-CH = CH-	E	5.81	−8.84	−1.96	18.42	3.709	−703.11
20	-CH = CH-	-CONH-	D	5.18	−8.83	−1.87	20.23	1.512	−1065.85
21	-S-	-CONH-	E	5.10	−8.94	−1.88	18.02	1.863	−853.94
22	-S-	-CO-	C	4.64	−8.88	−1.98	18.04	1.148	−848.97
23	-CH = CH-	-CONH-	E	4.26	−8.91	−1.77	18.05	2.126	−875.16
24	-S-	-CO-	B	4.22	−9.28	−1.62	15.64	4.11	−182.8
25	-CH = CH-	-CO-	C	4.10	−8.91	−2.01	18.15	1.41	−872.85
26	-CH = CH-	-CO-	B	4.05	−9.28	−1.59	15.75	4.371	−182.1
27	-S-	-CO-	D	3.85	−9.43	−2.00	17.94	1.718	−1044.88
28	-CH = CH-	-CO-	D	3.43	−9.56	−2.12	18.12	1.98	−1059.06
29	-S-	-CO-	E	3.22	−9.56	−2.08	16.88	2.253	−852.85
30	-CH = CH-	-CO-	E	2.84	−9.62	−2.11	16.59	2.514	−877.74

[a] R (coupling component):

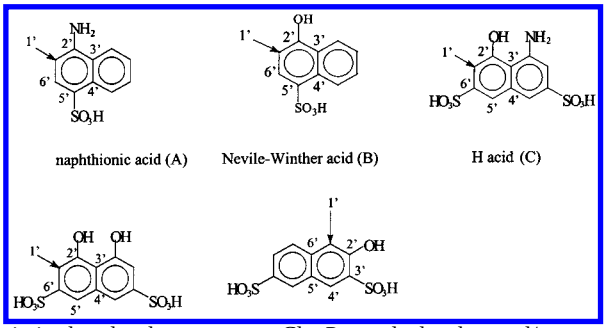

[b] L − molecular length derived from optimized molecular structures; ClogP − calculated ocanol/water partition coefficient; AM1 semiempirical quantum-mechanics results: E_{HOMO} − HOMO molecular orbital energy, E_{LUMO} − LUMO molecular orbital energy, ΔH - gas-phase molecular acidity.

moiety is in the trans configuration in azo derivatives.[22,23] For the lowest energy conformations, semiempirical molecular orbital calculations were carried out. The AM1 Hamiltonian[24] was employed by the MOPAC 93[25,26] software. Geometries were completely optimized by the eigenvector following routine.[27] For each compound the conformation of lowest energy was used in CoMFA calculations. The molecules were aligned according to the RMS_FIT option within SYBYL (compound 1 was considered as template). Three different alignment rules were studied. In the alignment rule ***a*** the following atoms were considered: the nitrogen atoms of the azo group plus the atoms C^1 and C^4 (see Table 1). The alignment rule ***b*** used the same atoms from rule ***a*** plus the atoms C^2, C^3, C^5, and C.[6] The alignment rule ***c*** used the atoms from rule ***b*** plus $C^{1'}$, $C^{2'}$, $C^{3'}$, $C^{4'}$, $C^{5'}$, and $C^{6'}$.

Six different alignment models were considered. In Alignment model 1, structures were built and optimized empirically using the Tripos 5.2 force field,[21] and partial charges were determined using the Gasteiger-Marsili (G−M) method,[28,29] as implemented in Sybyl 6.5. In alignment model 2, structures were built and optimized empirically using the Tripos 5.2 force field,[21] and partial charges were determined using the Gasteiger-Hückel (G−H) electronegativity-based method, as implemented in Sybyl 6.5. Alignment models 1−5 used neutral (N) molecules and alignment model 6 anionic (I) molecular structures (the anionic dye structures were built from the acidic (neutral) ones taking into account all the sulfonic acid group from the coupling component).

In the Alignment models 3−6, the structures were optimized using the AM1 semiempirical quantum-mechanics

Table 2. Summary of MLR Equations $-\Delta\mu_C^o = a + bX_1 + cX_2$[a]

	descriptors									
eq no.	X_1	X_2	a	b	c	r^2_{CV}	StdErr	r^2	F	relative contributions
1	E_{LUMO}		20.125	7.552		0.454	2.335	0.527	31.237	-
2	E_{HOMO}		79.664	8.165		0.581	2.032	0.642	50.182	-
3	ClogP		3.977	1.089		0.057	3.061	0.187	6.454	-
4	L		2.220	0.273		−0.089	3.374	0.014	0.353	-
5	ΔH		10.34	0.005		0.233	2.755	0.341	14.520	-
6	E_{HOMO}	V_W	96.297	8.15	−0.077	0.666	1.768	0.739	38.160	$0.721E_{HOMO}$; $0.279\ V_W$

[a] r^2 − conventional correlation coefficient; F − Fischer test; StdErr − standard errors of estimates; r^2_{CV} − leave-one-out "cross-validated r^2".

formalism. Each structure was optimized with the MOPAC 93[25] and partial atomic charges from the semiempirical AM1 method. Steric and electrostatic fields were computed using a sp^3 carbon with a charge probe of +1 as probe atom. Electrostatics was suppressed within the 30 kcal/mol steric energy cutoff.

A box with the dimensions 34 × 26 × 18 Å and a grid spacing of 2 Å were used. Statistical analysis was carried out by the PLS method[30] with the leave-one-out (LOO)[31] cross-validation procedure to determine the optimal number of components to be used in the final PLS analysis (without cross-validation). All the cross-validation calculations were performed with a minimal σ (column filter) value of 2.00 kcal/mol. "CoMFA STD" (block) scaling of independent variables within SYBYL was used for the steric and electrostatic fields.

Several molecular descriptors have been developed from dye three-dimensional structures and quantum-mechanics calculations. Thus, the molecular length (L) descriptor was derived from the AM1 optimized dye structures and measured between the extreme non-hydrogen atoms along the longest dye molecular axis. Dye hydrophobicity was expressed by the logarithm of the octanol/water partition coefficient and calculated by the ClogP software.[32] HOMO (E_{HOMO}), LUMO (E_{LUMO}) molecular orbital energies, and dipole moment were evaluated by quantum-mechanics calculations. Gas-phase acidity of the dye molecules was expressed as difference in the AM1 heats of formation of the anionic form and neutral form of the dyes, respectively

$$\Delta H = H_f(\text{anionic dye}) - H_f(\text{neutral dye})$$

omitting the constant H_f (H^+) for convenience.[33] The anionic dye structures were built from the acidic (neutral) ones taking into account the sulfonic acid group from the coupling component (in dye molecules with two sulfonic acid groups only the distal proton was removed from the acidic structures). Besides these descriptors the van der Waals volumes (V_W) were calculated by the additivity of van der Waals volume increments.[5] The MLR (Multiple Linear Regression) analysis has been performed by the SYSTAT program, version 5.03 (1991), from SYSTAT, Inc., Evenston, IL.

RESULTS AND DISCUSSION

Using descriptors described above correlations with the dye affinity have been established by multiple linear regressions. The QSAR equation and the corresponding statistical parameters are given in Table 2.

Better statistics were obtained for models incorporating HOMO molecular orbital energies when used as single parameter or together with the bulk van der Waals parameter. Correlation with the dye affinity was improved when the van der Waals parameter was added as an additional parameter. They also show higher dependence on the dye affinity for the HOMO (E_{HOMO}) than the LUMO (E_{LUMO}) molecular orbital energies. In the case of the HOMO energy, the correlation has a physical meaning if the dye acts as an electron donor of dye compounds at the cellulose/water interface. Electrical and nonelectrical attraction and repulsion forces act between dye cations and anions, respectively, and the negatively charged cellulose in the dyeing process.[35] It is considered that dye adsorption on textile fiber takes place only if attraction forces are dominant in the immediate vicinity of fiber surface.

The statistical results of equations with the other structural parameters indicate poor correlations with the dye affinity and predictability. Thus, attempts to correlate the adsorption strength with the ClogP hydrophobicity parameter showed poorer statistical results and apparently small relevance of difference in hydrophobic dye-cellulose interactions. Nonsatisfactory statistical results have been noticed with the molecular length descriptor (L), as opposed to the previous[9] correlations with this parameter. Poor statistical results were also obtained when gas-phase acidity (ΔH) was correlated with the dye affinity; intrinsic dye acidity does not influence the dye binding to the cellulose fiber.

A summary of the statistical results for several CoMFA models is presented in Tables 3 and 4. Cross-validation results (LOO) are presented in Table 3. Regression results from the best LOO models show that statistically significant

Table 3. Overview of Leave-One-Out Cross-Validation CoMFA Results[a]

no.	alignment models	# PCs	1	2	3	4	5
1	N, Tripos, G−M, ***a***	r^2_{CV}	0.266	0.394	0.491	0.499	0.499
		SDEP	2.910	2.692	2.515	2.544	2.666
2	N, Tripos, G−H, ***a***	r^2_{CV}	0.360	0.563	0.609	0.609	0.609
		SDEP	2.716	2.287	2.204	2.361	2.356
3	N, AM1, AM1, ***a***	r^2_{CV}	0.408	0.444	0.472	0.532	0.570
		SDEP	2.612	2.579	2.561	2.457	2.404
4	N, AM1, AM1, ***b***	r^2_{CV}	0.165	0.304	0.474	0.577	0.611
		SDEP	3.102	2.886	2.555	2.336	2.288
5	N, AM1, AM1, ***c***	r^2_{CV}	0.585	0.585	0.597	0.653	0.653
		SDEP	2.186	2.304	2.236	2.118	2.187
6	I, AM1, AM1, ***a***	r^2_{CV}	0.046	0.233	0.419	0.419	0.419
		SDEP	3.317	3.029	2.687	3.088	3.248

[a] r_{CV}^2- leave-one-out "cross-validated r^2"; SDEP − standard errors of predictions; alignment rule ***a*** includes the following atoms: the nitrogen atoms of the azo group plus the atoms C^1 and C^4 (see Table 1); alignment rule ***b*** used the same atoms from rule ***a*** plus the atoms C^2, C^3, C^5, and C;[6] alignment rule ***c*** used the atoms from rule ***b*** plus $C^{1'}$, $C^{2'}$, $C^{3'}$, $C^{4'}$, $C^{5'}$, and $C^{6'}$.

Table 4. Summary of CoMFA Regression Results[a]

alignment model	StdErr	r^2	F	relative contributions	
				steric	electrostatic
1	1.419	0.383 (3)	44.771	0.477	0.523
2	1.197	0.885 (3)	66.426	0.452	0.548
3	1.502	0.811 (2)	58.077	0.276	0.724
4	0.798	0.951 (4)	120.584	0.307	0.693
5	1.758	0.732 (1)	76.500	0.308	0.692
6	1.978	0.685 (3)	18.830	0.524	0.476

[a] r^2 − conventional correlational coefficient (the optimum PLS-component number used in the non-cross-validated PLS analysis is given in parentheses); F − Fischer test; SEE − standard errors of estimates.

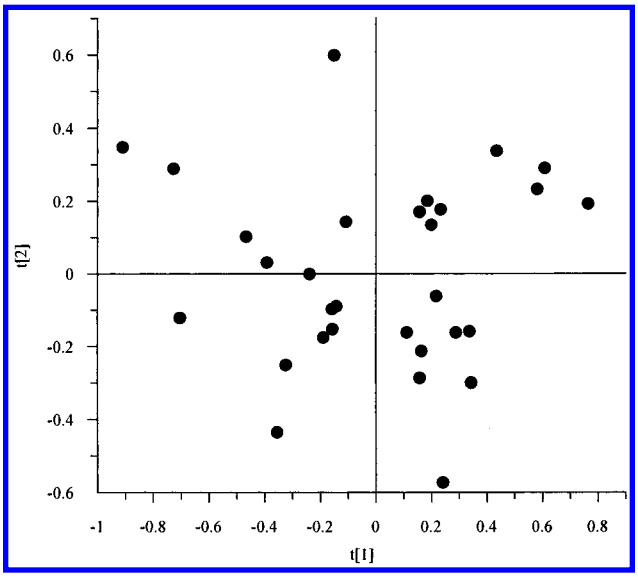

Figure 1. Plot of X-scores of the first two PLS-components according to the CoMFA model I (Alignment model 3).

correlations have been obtained (Table 4). Only two or three latent variables are required to establish a robust QSAR model.

Different CoMFA statistical results have been obtained for six alignment models. Sensitivity to the level of description in the alignment models has been noticed. A predictable model is considered Alignment model 3 with only two optimal PLS-components. This result favors the pharmacophoric hypothesis, which states that microcrystalline cellulose creates a binding site similar to the biological receptor binding site, which recognizes molecular patterns of dye molecules. It indicates a specific affinity of binding, opposite to previous findings,[9] even if it is less specific in

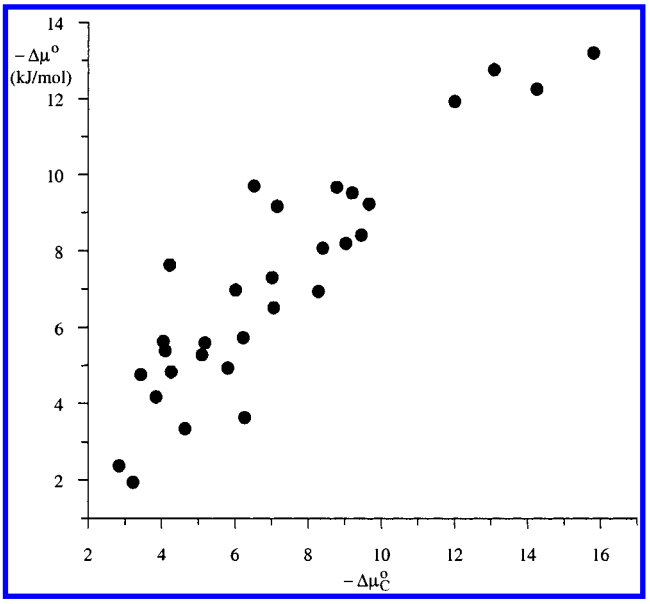

Figure 2. Plot of experimental ($-\Delta\mu^o$) versus calculated ($-\Delta\mu_C^o$) dye affinities for CoMFA model I (Alignment model 3).

comparison with ligand-biological receptor interactions. The X-score plot of the first two PLS-components is presented in Figure 1. The molecular dye structures obtained by this model are closer to the crystallographic information in comparison with Alignment models 1 and 2.

Inferior statistical results are noticed for Alignment model 6 with dye molecules as anionic structures.

In all the studied models (except Alignment model 6) the electrostatic field dominates the steric one (electrostatic dye-fiber interactions would be expected), in accordance with previous studies.[7,8,12] The actual versus predicted dye affinity plot is presented in Figure 1.

Table 5 presents results of statistical analysis when using additional quantum chemical descriptors such as the HOMO (E_{HOMO}) and LUMO (E_{LUMO}) molecular orbital energies, respectively, besides the steric and electrostatic CoMFA fields obtained in the Alignment model 3. The presence of the quantum chemical descriptors improved the correlation with dye affinity.

Good correlations with the dye affinity and predictions of compounds with higher affinities have been noticed for CoMFA model I from Table 5 (or Alignment model 3 in Table 4). In this model (see Table 5) only CoMFA (steric and electrostatic) fields were involved. The statistical results indicate the predominance of electrostatic effects in dye-cellulose fiber binding, as stated previously.[7,8] The predomi-

Table 5. CoMFA Statistical Results for Alignment Model 3 ("Cross-Validated r^2" (r_{CV}^2) and Standard Errors of Predictions (SEP) for the Optimum Number of PLS-Components; Conventional r^2, F-test, Standard Errors of Estimates (SEE), and Contributions (Normalized Coefficients and Fractions) of the Respective Structural Descriptors

model	type[a]	SDEP[b]	r_{CV}^2	StdErr	r^2	F	normalized coefficient[a]			fraction[a]		
							S	E	descriptors	S	E	descriptors
I	CoMFA (S, E)	2.579 (2)	0.444	1.502	0.811	58.08	0.739	1.941	-	0.276	0.724	-
II	CoMFA (S, E), E_{HOMO}	2.023 (2)	0.658	1.286	0.862	84.13	0.431	0.973	0.615 E_{HOMO}	0.214	0.482	0.305 E_{HOMO}
III	CoMFA (S, E), E_{LUMO}	2.153 (2)	0.612	1.649	0.773	45.89	0.457	0.749	0.590 E_{LUMO}	0.255	0.417	0.329 E_{LUMO}
IV	CoMFA (S, E), ΔH	2.306 (2)	0.555	1.766	0.736	37.69	0.348	0.944	0.509 ΔH	0.193	0.524	0.283 ΔH
V	CoMFA (S, E), E_{HOMO} E_{LUMO}	1.762 (1)	0.731	1.590	0.781	99.76	0.058	0.124	0.490 E_{HOMO} 0.444 E_{LUMO}	0.052	0.111	0.439 E_{HOMO} 0.398 E_{LUMO}

[a] S = steric field; E = electrostatic field; E_{HOMO} − HOMO molecular orbital energy; E_{LUMO} − LUMO molecular orbital energy, ΔH − gas-phase acidity. [b] The optimum PLS-component number used in the non-cross-validated PLS analysis is given in parentheses.

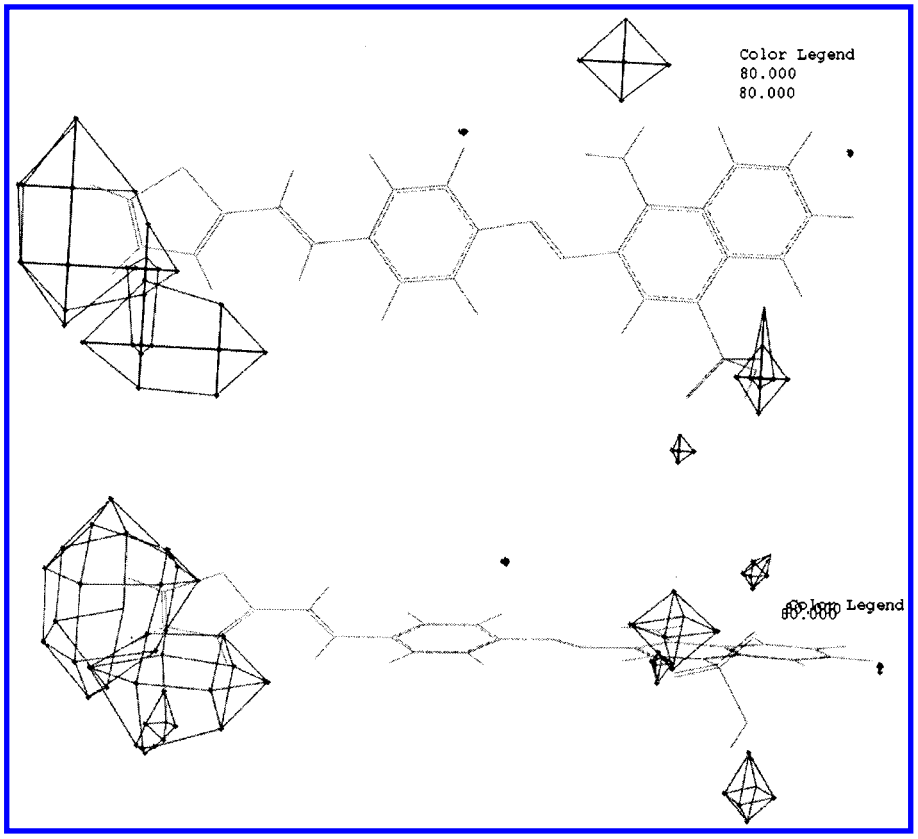

Figure 3. Top and side view of regions with sterically favorable interactions.

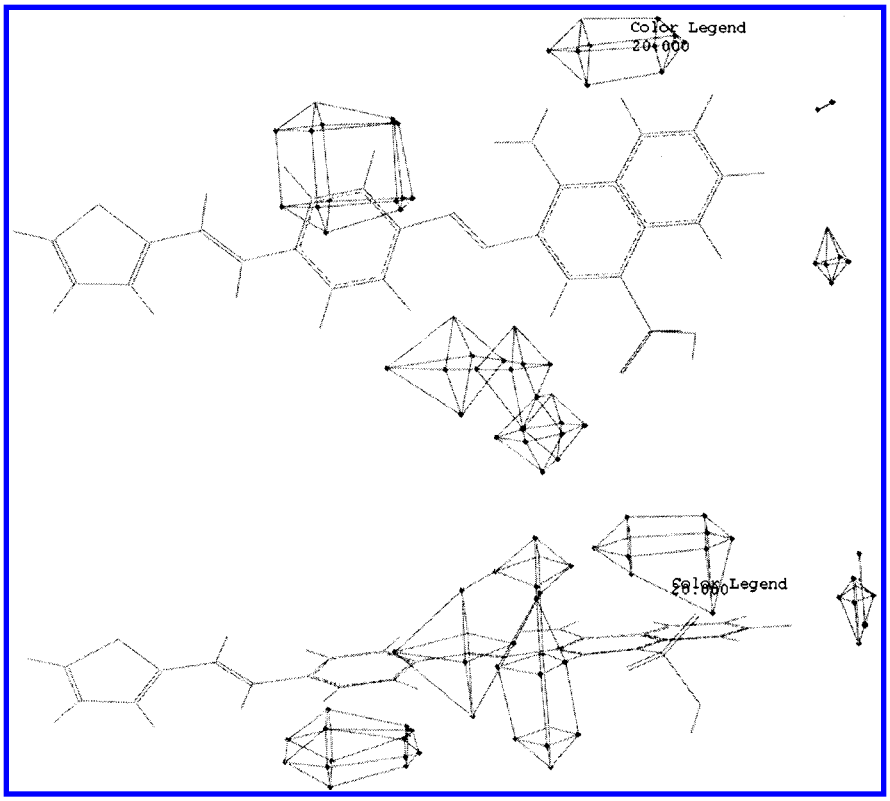

Figure 4. Top and side view of regions with sterically unfavorable interactions.

nance of the electrostatic field indicates polar attractions between the dye molecules and the fiber. The electrostatic coefficient contour maps indicate the predominance of positive over the negative charges. The introduction of the HOMO and LUMO molecular orbital energies, respectively, as independent variables, together with the CoMFA steric and electrostatic fields, increased significantly the quality of model I (see Table 5). Improvements in the statistical results have been noticed when HOMO molecular orbital energy was added as an independent variable to the CoMFA steric and electrostatic fields in model II. The inclusion of the HOMO molecular orbital energy in this model can be

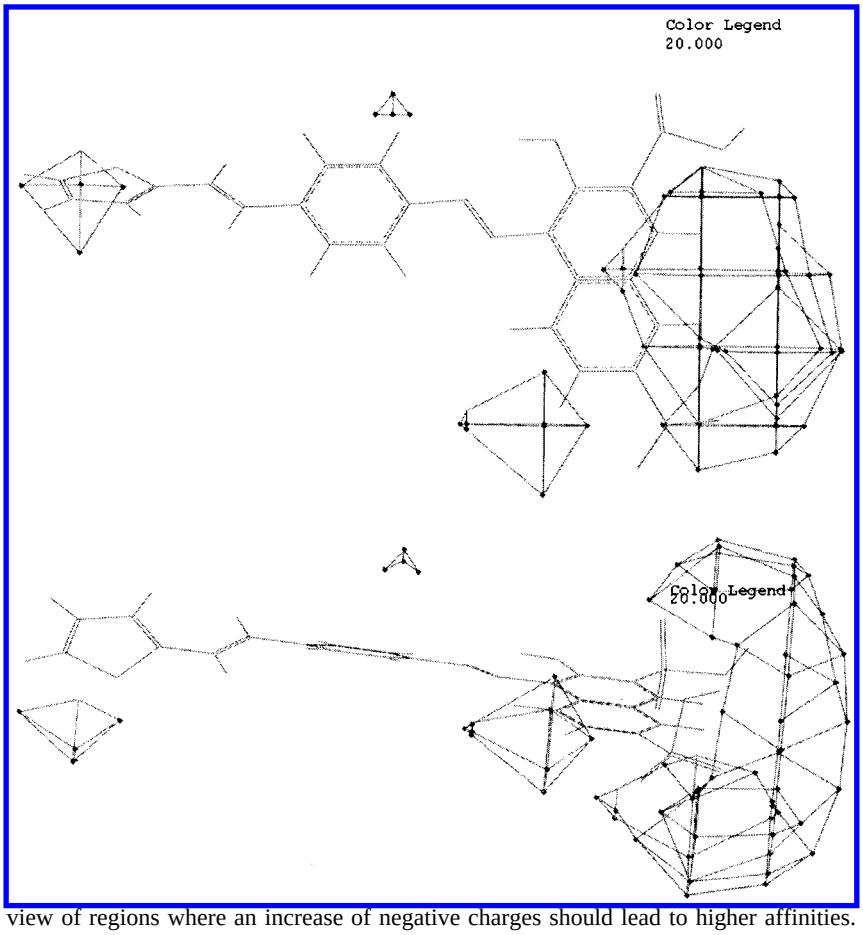

Figure 5. Top and side view of regions where an increase of negative charges should lead to higher affinities.

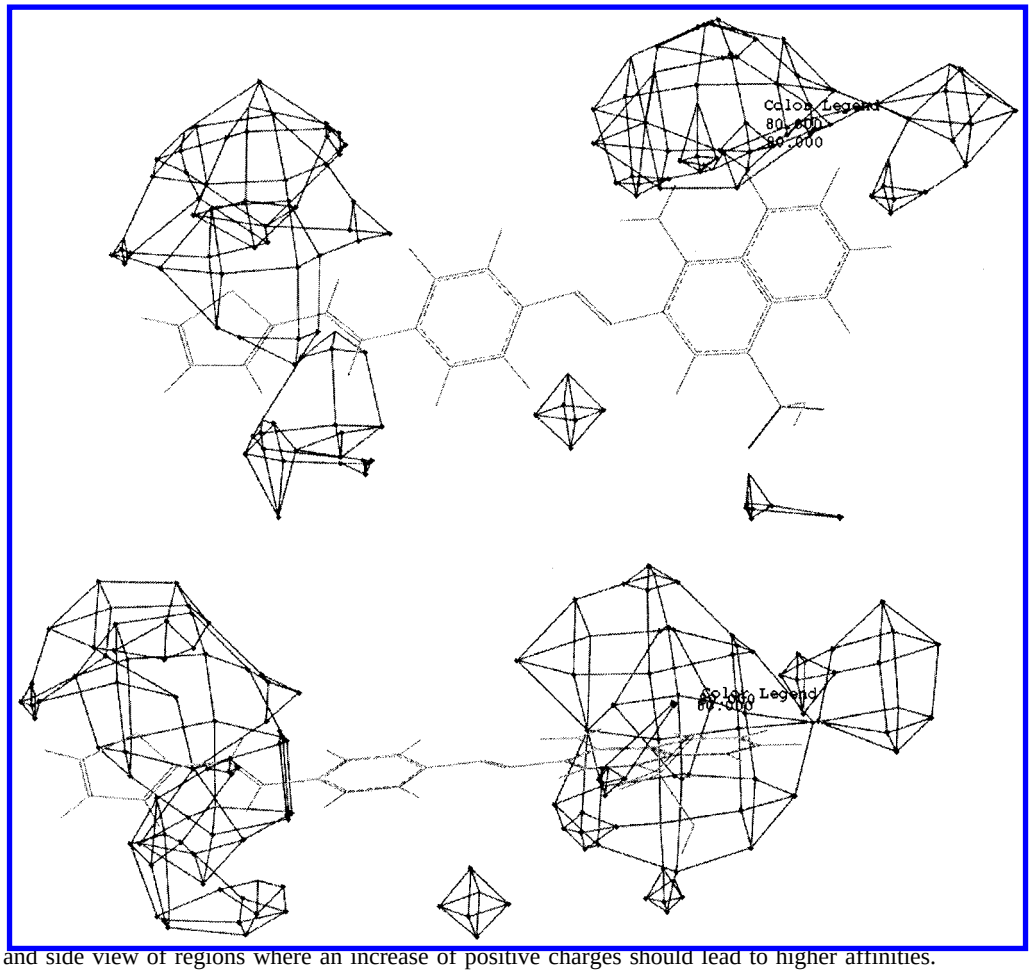

Figure 6. Top and side view of regions where an increase of positive charges should lead to higher affinities.

explained by the donor ability of the dye molecule in the dye adsorption on cellulose. The HOMO molecular orbital energy has a higher contribution to the dye affinity in comparison with the LUMO molecular orbital energy.

Inclusion of the LUMO molecular orbital energy, gas-phase acidity (ΔH) as well as HOMO and LUMO molecular orbital energies as additional variables together with the CoMFA electrostatic and steric fields (models III−V) did not yield better statistical results. In all models I−V, electrostatic interactions are dominant.

The dependence of the experimental vs calculated dye affinity for CoMFA model I (or Alignment model 3) is presented in Figure 1. Graphic results of the activity-contribution plots are presented in Figures 2−5. They indicate the dominant preponderance of electrostatic interactions in dye-cellulose binding in comparison with the steric ones. The coefficient contour maps for the steric field of model I are presented in Figures 2 and 3. Contour levels for both negative and positive contributions were set to 0.8. Favorable for dye adsorption on cellulose would be bulk heterocyclic substituents (the beneficial area has more importance as more points are distributed in the surrounding heterocyclic region, including the bridge to the phenyl moiety). Increased bulk substituents in the ortho position relative to the azo group in R or chromotropic acid when used as a coupling component are unfavorable for dye-cellulose binding.

Negative charges in the coupling components (due to the sulfonic acid groups) are implied in the first steps of dye solubilization in the dyeing environment, being favorable to the dye adsorption on cellulose. Increased positive local charges extended on side areas of molecules are favorable to the dye binding on negatively charged cellulose,[34] in accordance with previous studies.[18]

The contour plots indicate that increased affinity for cellulose fiber would be obtained for dyes having increased heterocyclic moiety and substituents able to increase the positive local charges in the molecule.

CONCLUSIONS

Quantitative structure−activity relationship (QSAR) models for a series of 30 anionic azo dyes applied to cellulose fiber have been studied by comparative molecular field analysis. Two forms of the dye molecules (neutral and anionic) are compared. Neutral structures give better statistical results than the anionic species. The electronic and structural properties of these dyes were calculated by the semiempirical AM1 method. Several alignment rules have been considered in the CoMFA calculations. Sensitivity to the level of description in the alignment models has been noticed. It indicates a specific affinity of binding in terms of pharmacophoric constraints, even if it is less specific in comparison with ligand-biological receptor interactions. The CoMFA results indicate the predominance of electrostatic interactions in dye-cellulose binding. The dominant contribution of the HOMO orbital molecular energy, used as descriptor, can be explained by the donor ability of the dye compounds at the cellulose/water interface. Local positive charges of dye molecules are favorable for adsorption on negatively charged cellulose.

ACKNOWLEDGMENT

Financial support for a research stay of Simona Funar-Timofei at Leipzig from the Saxon Ministry of Science and Arts, reference no. 7531.50-04-840-98/2, is gratefully acknowledged.

REFERENCES AND NOTES

(1) Timofei, S.; Schmidt, W.; Kurunczi, L.; Simon Z.; Sallo, A. A QSAR Study of the Adsorption by Cellulose Fibre of Anthraquinone Vat Dyes. *Dyes Pigm.* **1994**, *24*, 267−279.

(2) Timofei, S.; Kurunczi, L.; Schmidt, W.; Fabian, W. M. F.; Simon, Z. Structure-Affinity Binding Relationships by Principal-Component-Regression Analysis of Anthraquinone Dyes. *Quant. Struct.-Act. Relat.* **1995**, *14*, 444−449.

(3) Timofei, S.; Kurunczi, L.; Schmidt, W.; Simon, Z. Structure-Affinity Binding Relationships of Some 4-Aminoazobenzene Derivatives for Cellulose Fibre. *Dyes Pigm.* **1995**, *29*, 251−258.

(4) Timofei, S.; Kurunczi, L.; Schmidt, W.; Simon, Z. Dye Structure-Affinity Relationships by the MTD Method. *Rev. Roum. Chim.* **1997**, *42*, 687−692.

(5) Timofei, S.; Kurunczi, L.; Schmidt, W.; Simon, Z. Lipophilicity in Dye-Cellulose Fibre Binding. *Dyes Pigm.* **1996**, *32*, 25−42.

(6) Timofei, S.; Kurunczi, L. In *Quantitative Relationships between Chemical Structure and Biological Activity (QSAR). The MTD Method*; Chiriac, A., Ciubotariu, D., Simon, Z., Eds.; Mirton Publishing House: Timişoara, 1996; pp 205−220.

(7) Fabian, W. M. F.; Timofei, S.; Kurunczi, L. Comparative Molecular Field Analysis (CoMFA), Semiempirical (AM1) Molecular Orbital and Multiconformational Minimal Steric Difference (MTD) Calculation of Anthraquinone Dye-Fibre Affinities. *J. Mol. Struct., THEOCHEM* **1995**, *340*, 73−81.

(8) Fabian, W. M. F.; Timofei, S. Comparative molecular field analysis (CoMFA) of dye-fibre affinities II: symmetrical bisazo dyes. *J. Mol. Struct., THEOCHEM* **1996**, *362*, 155−162.

(9) Oprea, T. I.; Kurunczi, L.; Timofei, S. QSAR Studies of Disperse Azo Dyes. Towards the Negation of The Pharmacophore Theory of Dye-Fibre Interaction? *Dyes Pigm.* **1997**, *33*, 41−64.

(10) Timofei, S.; Schmidt, W.; Kurunczi, L.; Simon, Z. A Review of QSAR for Dye Affinity for Cellulose Fibres. *Dyes Pigm.* **2000**, *47*, 5−16.

(11) Cramer III, R. D.; Patterson, D. E.; Bunce, J. D. Comparative Molecular Field Analysis (CoMFA). 1. Effect of Shape on Binding of Steroids to Carrier Proteins. *J. Am. Chem. Soc.* **1988**, *110*, 5959−5967.

(12) Timofei, S.; Fabian, W. M. F. Comparative Molecular Field Analysis (CoMFA) of Heterocyclic Monoazo Dye-Fibre Affinities. *J. Chem. Inf. Comput. Sci.* **1998**, *38*, 1218−1222.

(13) Woodcock, S.; Henrissat, B.; Sugiyama, J. Docking of Congo Red to the Surface of Crystalline Cellulose Using Molecular Mechanics. *Biopolymers* **1995**, *36*, 201−210.

(14) Vieira Ferreira, L. F.; Garcia, A. R.; Rosário Freixo, M.; Costa, S. M. B. Photochemistry on Surfaces: Solvent-Matrix Effect on the Swelling of Cellulose. *J. Chem. Soc., Faraday Trans.* **1993**, *89*, 1937−1944.

(15) Mondal, I. H.; Kai, A. Structure of Nascent Microbial Cellulose I. Effects of Methyl and Methoxy Groups of Direct Blue 1 and 53 on Nascent Microbial Cellulose. *Polym. J.* **1998**, *30*, 78−83.

(16) Kai, A.; Mondal, I. H. Influence of substituent of direct dye having bisphenylenebis(azo) skeletal structure on structure of nascent cellulose produced by Acetobacter xylinum [I]: different influence of Direct Red 28, Blue 1 and 15 on nascent cellulose. *Int. J. Biol. Macrom.* **1997**, *20*, 221−231.

(17) French, A. D.; Battista, O. A.; Cuculo, J. A.; Gray, D. G. In *Kirk-Othmer Encyclopedia of Chemical Technology*; 4th ed.; Wiley: New York, 1993; Vol. 5, p 476.

(18) Nugmanov, O. K.; Pertsin, A. I.; Zabelin, L. V.; Marchenko, G. N. Molekulyarno − kristalicheskaya struktura tselyulozy. *Usp. Khim.* **1987**, *56*, 1339−1359.

(19) Fisichella, S.; Scarlata, G.; Torre, M. Correlation between R_m and Standard Affinity of Some Anionic Azo Dyes on Cellulose. *J. Soc. Dyers Colour.* **1978**, *94*, 521−523.

(20) SYBYL 6.5; Tripos Associates, St. Louis, MO.

(21) Clark, M.; Cramer III, R. D.; van Opdenbosch, N. Validation of the General Purpose Tripos 5.2 Force Field. *J. Comput. Chem.* **1989**, *10*, 982−1012.

(22) Gilardi, R. D.; Karle, I. L. The Crystal Structure of 4-Phenylazo-azobenzene. *Acta Crystallogr., B* **1972**, *28*, 1635−1638.

(23) Hanson, A. W. The Crystal Structure of Methyl Orange Monohydrate Monoethanolate. *Acta Crystallogr., B* **1973**, *29*, 454−460.

(24) Dewar, M. J. S.; Zoebisch, E. G.; Healy, E. F.; Stewart, J. J. P. A New General Purpose Quantum Mechanical Molecular Model. *J. Am. Chem. Soc*. **1985**, *107*, 3902−3909.
(25) Stewart, J. J. P. MOPAC: A semiempirical molecular orbital program. *J. Comput.-Aided Mol. Des.* **1990**, *4*, 1−105.
(26) Mopac 93; Fujitsu Limited, 9-3, Nagase 1-Chome, Mihama-ku, Chiba-city, Chiba 261, Japan, and Stewart Computational Chemistry, 15210 Paddington Circle, Colorado Sprongs, CO 80921, U.S.A., 1993.
(27) Baker, J. Algorithm for the Location of Transition States. *J. Comput. Chem.* **1986**, *7*, 385−395.
(28) Gasteiger, J.; Marsili, M. Iterative partial equalization of orbital electronegativity: a rapid access to atomic charges. *Tetrahedron* **1980**, *36*, 3219−3222.
(29) Marsili, M.; Gasteiger, J. π Charge distribution from molecular topology and π orbital electronegativity. *Croat. Chem. Acta* **1980**, *53*, 601−614.
(30) Wold, S.; Ruhe, A.; Wold, H.; Dunn, W. J., III The Collinearity Problem in Linear Regression. The Partial Least Squares (PLS) Approach to Generalized Inverses. *SIAM J. Sci. Stat. Comput.* **1984**, *5*, 735−743.
(31) Cramer, R. D.; Bunce, J. D.; Patterson, D. E.; Frank, I. E. Crossvalidation, Bootstraping, and Partial Least Squares Compared with Multiple Regression in Conventional QSAR Studies. *Quant. Struct.-Act. Relat.* **1988**, *7*, 18−25.
(32) ClogP, version 1.0.0; BioByte Corp., Claremont, CA, U.S.A.
(33) Schüürmann, G. Modelling pK_a of Carboxylic Acids and Chlorinated Phenols. *Quant. Struct.-Act. Relat*. **1996**, *15*, 121−132.
(34) Rattee I. D. The Role of Water in Dyeing. *J. Soc. Dyers Colour*. **1974**, *(10)*, 367−372.
(35) Vickerstaff, T. *The Physical Chemistry of Dyeing*; Imperial Chemical Industries Limited: London, 1954.

CI010086V